Win-win possibilities through capacity tariffs and battery storage in microgrids

Kevin Milis[a,*], Herbert Peremans[a], Johan Springael[a], Steven Van Passel[a,b]

[a] *Department of Engineering Management, Faculty of Applied Economics, University of Antwerp, Belgium*
[b] *Centre for Environmental Sciences, Hasselt University, Hasselt, Belgium*

Abstract

This paper investigates the impact of capacity tariff design on microgrids. While the possible benefits for utilities of capacity tariffs are well researched, comparatively little work has been done investigating the effects of capacity pricing on prosumers. Through simulating a grid connected microgrid and solving the day-ahead dispatch problem for a calendar year, we show that a well-designed capacity tariff will not only smooth out demand profiles, but could also lead to less erratic charge/discharge cycles in a real-time pricing scenario, lessening battery degradation. These results show that a properly designed capacity tariff has the potential to be beneficial for both the utilities as well as the battery-owning prosumer. Furthermore, we propose a new, heuristic approach to solve the day-ahead economic dispatch problem, which we prove to be effective and efficient. Additionally, we demonstrate that our novel approach does not impose mathematical restrictions such as continuous differentiability of the objective function. We show that the proposed capacity tariff achieves the stated aim of promoting battery storage uptake and that our novel method allows for compression and shorter run times.

Keywords: battery storage, microgrid, economic optimisation, heuristic

*Corresponding author
Email addresses: kevin.milis@uantwerpen.be (Kevin Milis), herbert.peremans@uantwerpen.be (Herbert Peremans), johan.springael@uantwerpen.be (Johan Springael), steven.vanpassel@uantwerpen.be (Steven Van Passel)

Nomenclature

Symbol	Meaning
$Q_g(t)$	Amount of energy bought from the grid during time step t, in kWh
$Q_s(t)$	Amount of energy withdrawn from storage during time step t, in kWh
$Q_{s,0}$	Amount of energy in storage at the start of the optimization window, in kWh
$Q_{s,max}$	Maximum battery capacity, in kWh
$Q_i(t)$	Amount of energy available from intermittent generation during time step t, in kWh
$Q_l(t)$	Load to be served during time step t, in kWh
$P_g(t)$	Price of grid electricity during time step t, in €$/kWh$
C_{p1}	Capacity price of the first capacity block, in €$/kW$
C_{p2}	Capacity price of the second capacity block, in €$/kW$
C_{bar}	Upper limit of the first capacity block, in kW
H	Length of optimization window, in hours
S	State of charge of the battery, in kW
l	Rate of self-discharge of the battery, in $\%/h$

Highlights

- Heuristic day-ahead dispatch method proposed
- Method allows for reduced computation time without overly impacting solution quality
- Electricity capacity tariff shown beneficial both for utilities and consumers

1. Introduction

This paper investigates the impact of capacity tariff design on microgrids in general, with a particular focus on how the economics of storage in microgrids are impacted, using a simulation and optimisation approach. After elaborating on the motivation behind this research, an overview of relevant research is provided, while an overview of the research hypotheses and the contributions of the work closes this section. The second section provides a comprehensive overview of the heuristic solution method used and also describes the simulation set-up used in detail. A discussion of the obtained results in presented in the third section of this paper, while the fourth section summarizes the most important findings and highlights avenues of further research.

1.1. Background and motivation

A microgrid is defined in [1] as "a group of interconnected loads and distributed energy resources within clearly defined electrical boundaries, that acts as a single controllable entity with respect to the grid". Furthermore it is also stipulated in [1] that such a microgrid should be able to both connect to and disconnect from the grid as needed, meaning a microgrid can work connected to the grid, but also in island mode.

Previous work [2] has shown that the reported profitability for energy storage systems, and specifically batteries, as part of a microgrid is negative. This means that said batteries do not generate economic value and are hence not included in a cost-optimal system configuration, under the researched conditions. Contrast this with the finding that batteries will be needed to allow for more integration of renewable energy [3].

It is this apparent mismatch between reported private economic outcomes on the one hand and forecast public benefits on the other hand that forms the main motivation for this research. The aim of this study is to investigate if a capacity tariff for electricity could help steer microgrids towards the uptake of batteries.

1.2. Literature review

Microgrids are an increasingly active area of scientific study. A large body of work focusses on more technical aspects, see for example [4], which discusses how the spinning reserve of an isolated microgrid can be maximized. Contrast this with the work of Quashie et al. [5] where the topic is also the reserve capacity of a microgrid, but now against the backdrop of cooperation with the distribution system operator. Returning to the case of isolated microgrids, [6] expounds how to assure stability in an islanded microgrid, while other authors focus their research on more specific parts of a microgrid [7]. Interestingly, while still maintaining a mostly technical focus, recent work [8] looks at the emergence

of clusters of microgrids connected to the main grid. This shifts the focus away from studying a single microgrid and its interaction with the grid.

However, not all research done on microgrids focuses on these technical aspects, as a framework categorizing end users' key energy service needs has been developed [9]. There is also a growing body of research literature that focusses on the economics surrounding microgrids: energy market design specifically for microgrids is investigated in [10]. The research interest in microgrids is spread across the globe: see [11] for a case study in Pakistan, or [12] for a discussion of three different projects in China. A wider look at the drivers and possible problems facing microgrids is given in [13], an issue which is also tackled in [14]. However, comparatively little work has been done where the impact of policy on microgrid economics are concerned [2], with most prior work focussing on carbon taxation, such as in [15].

Tariff design and its impact on microgrids is also a fruitful area of research, albeit with a narrow scope. The focus is almost entirely on feed-in tariffs: a review for Australia is provided in [16], and a comparison between feed-in tariffs and auctioning mechanisms as a way to promote renewable energy sources is presented in [17]. A feed-in tariff is included as one of several measures to promote storage systems as part of the power system for islands in [18], alongside R&D grants and investment subsidies.

If the focus on microgrids or renewable energy is relaxed, studies on different electricity tariffs are more prevalent: [19] is a study for Denmark, investigating the impact of different electricity tariffs in order to stimulate flexibility. This flexibility is provided by electric boilers in this study, but the findings are that a tariff design that moves away from purely volumetric tariffs can help speed up the integration of renewable energy systems. Similarly, [20] looks at the impact of electricity tariff design on flexible power to heat for a district heating network.

Methodologically, the problem of how to operate a microgrid at the lowest possible cost is usually formulated as a day ahead dispatch problem. This day ahead dispatch problem is in itself a well studied problem for a wide array of different energy-related applications: see [21] for a discussion of day ahead dispatch concerning electrical vehicles providing ancilary services, or [22] for an application in the scheduling of wind farms. One way to solve the optimisation problem corresponding with day head dispatch are heuristic methods[23], like a best improvement strategy or a first improvement strategy. Both of these heuristics are widely used to solve numerous optimization problems, see [24] for a comparissons of both strategies applied on a different problem and [25] for a more theoretical discussion of these two improvement strategies.

These simple heuristic methods have however found little headway when it comes to the solution of the day ahead dispatch problem in microgrids,as the most used methods are either commercially available software, such as HOMER, or more complex algorithms such as simulated annealing or particle swarm optimisation [26], even though the scientific validity of such techniques has been called into question [27].

Dimensionality reduction and compression of the solution space are techniques with are prevelant in computationally very heavy domains, such as for example image processing [28]. However they are also beginning to find traction in the broader field of sustainability, as noted in the review of Evins [29]. That being said, not many other references can be found of such techniques being used in microgrid or sustainability related topics, which tentatively supports the conclusion that these techniques are currently not being widelyb used in this field, despite the proven benefits they have offered in other fields [28].

1.3. Research hypothesis and contribution

The preceding literature review shows that there is clearly a need for more research focused on how to promote the uptake of battery systems. In that

regard, this study aligns itself with more economically focused research on microgrids. It fills the research gap outlined above, by investigating the impacts of different electricity tariff designs on microgrids, as these tariff designs have proven themselves to be effective in related areas.

In order to address this question, we propose a relatively simple heuristic solution method, based on the inherent periodicity present in residential load patterns. To the best of the author's knowledge, such an easily understandable heuristic has not been extensively used before when it comes to the day ahead dispatch problem for microgrids. The first tested hypothesis is whether a capacity tariff would prove to be beneficial for the adoption of battery storage. A second hypothesis is of a more methodological nature. We hypothesize that use can be made of the structure inherently present in the problem due to the periodical patterns present in the exogenous data sets. Specifically, we will investigate whether this structure can be utilized in a way that allows for shorter computational time.

The contributions of our work are twofold. Firstly, our results show that the implementation of a capacity tariff not only promotes the adoption of batteries by microgrids, but also has societal benefits in the shape of less strain on the electrical grid infrastructure. Furthermore, our results show that it is reasonable to assume that a capacity tariff will also have a positive impact on battery lifetime. Secondly, our proposed method allows for compression of the solution space, meaning solutions can be found more quickly.

2. Methods

This section starts by elaborating on the problem formulation; outlining both the simulation model used and the optimization problem to be solved. The second subsection shows our proposed solution method. Finally, the last

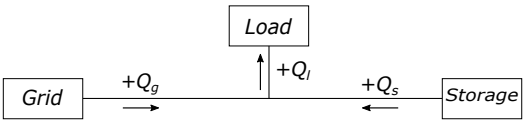

(a) Model without intermittent generation

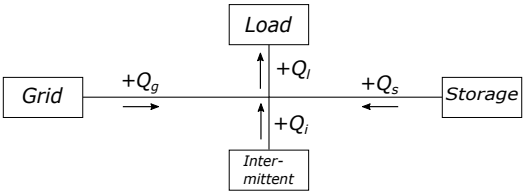

(b) Model with intermittent generation

Figure 1: Model configurations, reused from [30] with permission

subsection details the set-up of the experiments.

2.1. Problem formulation

Consider the economic dispatch problem for a grid connected microgrid. Our model, as shown in fig. 1 encompasses exogenous load, battery storage, and possibly exogenously driven local intermittent generation. Specifically, we determine the amount of electricity sold to or bought from the main grid that will minimize operating costs over a rolling window with a variable horizon H. The optimization problem is solved for the first horizon-length set of hours of the year, after which the obtained solution for the first hour is saved. Then, the optimization problem is solved for the next horizon window, but now starting with hour two of the year, as opposed to hour one. Again, the solution for the first hour, i.e. hour two of the year, is kept. This process is repeated until a solution has been found for the entire year.

The operating cost, to be minimised, has two components: an energy component, and a capacity component. The energy component is the product of a) the amount of energy withdrawn from or injected into the grid over one hour, $Q_g(t)$, and b) the price for energy during that hour, $P_g(t)$. This price can either be determined by fixed pricing, time of use pricing, or real time market pricing.

The capacity component of the cost function reflects a capacity block pricing scheme, based on the work of Schreiber et al. [34]. All capacity used up to a certain level C_{bar} will be paid at a rate C_{p1} and all capacity used above this level is charged at the higher rate C_{p2}. We choose to use this specific design since Schreiber et al. reported the best results with this kind of capacity market design in [34].

While the energy costs might be negative, reflecting a net benefit for the microgrid as it sells excess electricity to the main grid, the capacity component of the cost function will always be positive. This is by design, since injecting electricity into the main grid uses the same infrastructure as withdrawing energy from the grid. Due to the granularity of one hour and our assumption that the electric power withdrawn from, or injected to the grid is uniform within each hour, Q_g represents both the amount of energy, in kWh, as well as the peak load, in kW.

$$\min_{g_h} \left[\sum_{h=1}^{H} g_h \cdot \bar{b}_h \cdot \bar{P}_g + |\sum_{h=1}^{H} g_h \cdot \bar{b}_h| \cdot \bar{C}_{p1} + max(|\sum_{h=1}^{H} g_h \cdot \bar{b}_h| - \bar{C}_{bar}, 0) \cdot (\bar{C}_{p2} - \bar{C}_{p1}) \right] \tag{1}$$

Subject to

$$\bar{Q}_l = \sum_{h=1}^{H} g_h \cdot \bar{b}_h + \sum_{h=1}^{H} s_h \cdot \bar{b}_h + \bar{Q}_i \tag{2}$$

$$Q_{s,0} - \sum_{\tau=1}^{t} \sum_{h=1}^{H} s_h \cdot \bar{b}_h(\tau) \cdot e^{l \cdot \tau} \leqslant Q_{s,max} \cdot e^{l \cdot t} \quad \forall t = 1, \cdots, H \tag{3}$$

$$\sum_{\tau=1}^{t} \sum_{h=1}^{H} s_h \cdot \bar{b}_h(\tau) \cdot e^{l \cdot \tau} \leqslant Q_{s,0} \forall t = 1, \cdots, H \tag{4}$$

The formulation of the optimisation problem to be solved is given by eqs. (1) to (4). As full details on the derivation and particularities of this formulation can be found in appendix A, it suffices to note that eq. 1 is the objective function

to be minimized, eq. 2 is Kirchoff's current law for the single node depicted in fig. 1, and eqs. 3 and 4 respectively are the constraints on the charging and discharging of the battery. In equations (3) and (4), $\bar{b}_h(\tau)$ denotes the $\tau - th$ element of the $h - th$ basis vector. Additionally, all of the assumed exogenous variables in the model have been represented as vectors for consistency. $\bar{P}_g$, $\bar{Q}_l$ and $\bar{Q}_i$ each contain H values of the corresponding dataset for each of the H hours of the considered time period, while $\bar{C}_{p1}$, $\bar{C}_{p2}$ and $\bar{C}_{bar}$ are all size H vectors, with all elements being equal to C_{p1}, C_{p2} and C_{bar} respectively. All the products in equation (1) between vectors are scalar products.

2.2. Heuristic solution method

It is our goal to investigate whether it is possible to solve the economic dispatch problem for a microgrid, as outlined by equations (1) to (4), with a subset of basis vectors. Ideally, this compression should allow for shorter run times of the algorithm, depending on which components are kept and discarded during the compression step. However, the compression should also maintain a similar economic performance in terms of cost, in comparison with the same algorithm without compression. In order to get insight, we implemented a heuristic solver, in such a manner that we have full control over the algorithm. We solved the economic dispatch problem in three different bases to test the hypothesis with regard to the choice of basis impacting the quality of the compression.

The following subsections elaborate on our solution method: a first subsection shows the implemented heuristic. The next subsection details the different bases, used to solve the problem, while a final subsection outlines the set-up of the different simulations.

2.2.1. Heuristic search

We implemented a multi-start heuristic to solve the problem outlined above using a best improvement strategy. This strategy is depicted schematically in fig. 2. Best improvement evaluates h pairs of candidate solutions per optimization

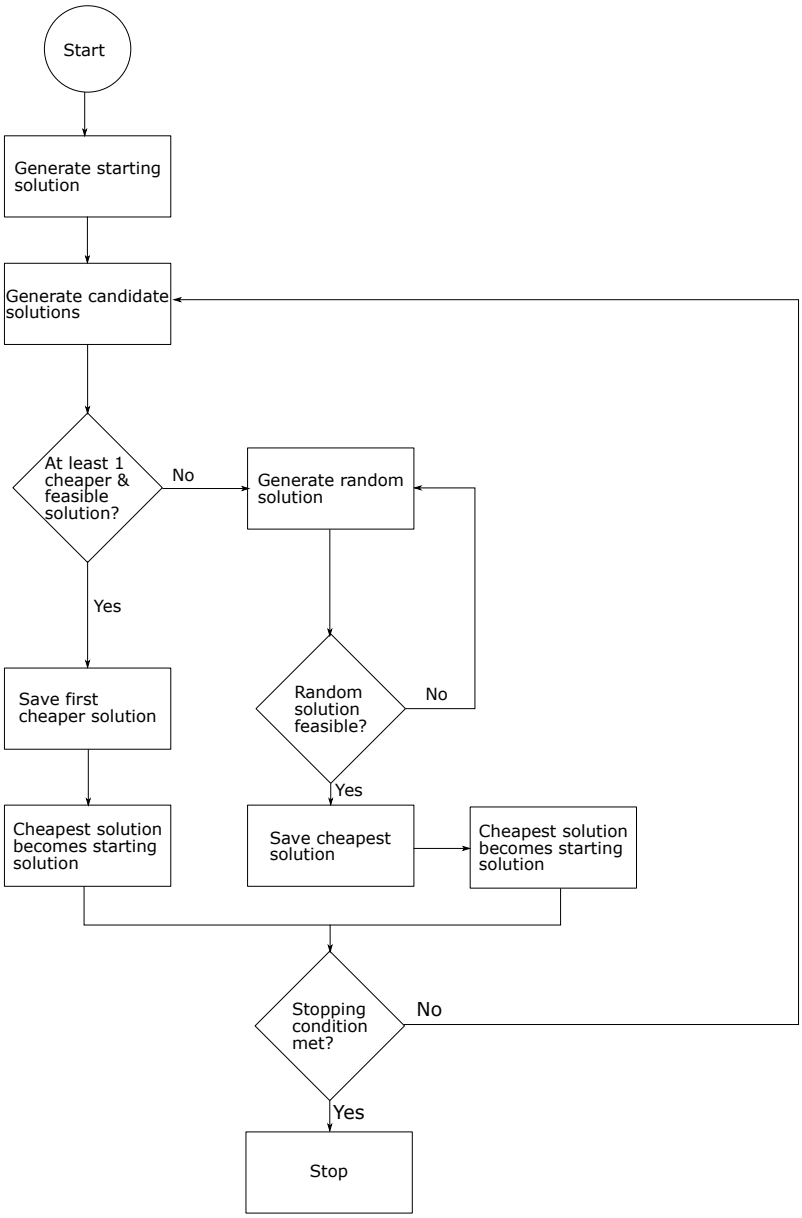

Figure 2: Heuristic flowchart

step, consisting of a positive and a negative step in each of the basis directions. If none of the evaluated solutions have a lower cost than the previous solution -or start solution, for the first iteration-, a random feasible solution is generated. The corresponding cost is calculated and the new solution is used as starting point for the next iteration. If there is at least one of the candidate solutions feasible with a lower cost, the feasible solution with the lowest cost will be selected. The heuristic runs through the optimization steps until one of two stopping criteria is met. The heuristic will stop after either a defined maximum number of iterations have been reached, or when the difference between the best solution found until now and the current solution is smaller than a certain threshold precision.

2.2.2. Bases

One of the hypotheses to be tested is whether or not exploiting the structure present in the problem impacts the operation of the algorithm used, leading to either cheaper solutions, or similar solutions found with less computational time elapsed. A natural candidate basis to investigate this is the sequentially ordered Walsh matrix of order h. Each of the columns of the matrix is taken as one of the h basis vectors, as each column has an increasing amount of sign switches as can be seen in fig. 3a. In our model, this corresponds to a higher frequency of switching between charge and discharge. This means that some of the patterns that one would expect to find in the solution are already present in the base matrix, such as the first basis vector providing for the constantly present base load, while the second basis term is well suited to model usage patterns with a periodicity of 8 hours, such as a working day.

However, Walsh matrices only exists for orders equal to powers of 2, meaning that there is no Walsh matrix of order 24, which is the usual time horizon considered for economic dispatch problems. As the time horizon for which we solve our optimization problem is flexible, this is not inherently a problem: the basis formed by the Walsh matrix of order 16 can be used to solve the optimization

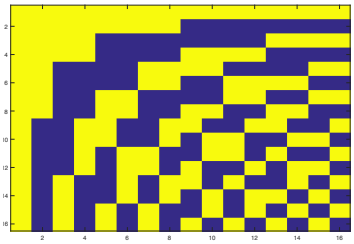

(a) Walsh matrix of order 16

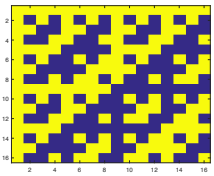

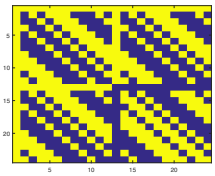

(b) Hadamard matrix of order 16 (c) Hadamard matrix of order 24

Figure 3: Overview of the different bases. Yellow cells correspond to a value of one, blue cells to a value of minus one.

problem, and is therefore one of the bases used in this paper.

Additionally, if we are willing to forgo the increasing amount of sign changes per column, the Hadamard matrix is similar to the Walsh matrix: compare for instance fig. 3a with fig. 3b and note that the Walsh matrix contains a large range of sign changes per column, whereas the corresponding Hadamard matrix does not. In order to construct a Hadamard matrix, it is only required that order of the matrix is even, meaning that a Hadamard matrix of order 24 can be used as a basis to solve the economic dispatch problem for a twenty-four hour time horizon.

As is clear from the comparison between figs. 3a, 3b and 3c, while the pattern of increasing sign changes is still somewhat present in the Hadamard matrix of order 16, it is almost completely gone from the Hadamard matrix of order 24. We use both Hadamard matrices as a basis as the comparison between the results of the Walsh and Hadamard matrix of order 16 will grant insight whether the sequential ordering is important, and comparing between the results obtained with the Hadamard matrix of order 16 and the Hadamard matrix of order 24 allows for the investigation of the impact of the chosen horizon on the outcome of the optimization.

Finally, for each of the considered time horizons, the standard basis, based on the identity matrix of the corresponding order of that dimension was also used. This provides a baseline against which performance of the other bases can be compared to, both in terms of number of iterations as in terms of total operating costs.

2.3. Simulation set-up

We solve the optimization problem outlined in eqs. (1) to (4) for a median Belgian household with an annual electricity demand of 3600 kWh. The stor-

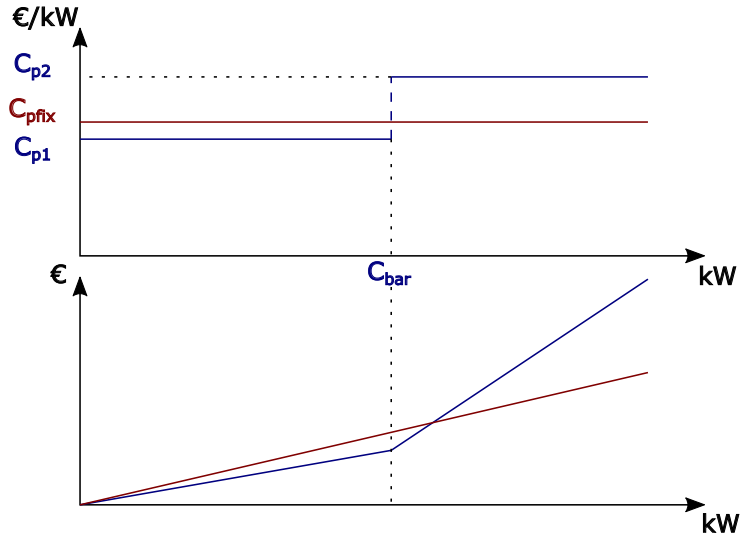

Figure 4: Schematic representation of block capacity (C_{p1}, C_{p2}) and fixed (C_{pfix}) capacity tariff depicting capacity tariff height (above) and resulting total capacity tariff payment (below) as a function of used capacity. Own composition based on [34].

age component is modeled after the Tesla Powerwall and sized at a maximum capacity of 7 kWh. In the literature, self discharge rates for Li-Ion batteries are reported between 5% and 10%, but these are always reported for a twenty-four hour period at minimum. To arrive at a 10% discharge after 24 hours, the discharge in our simulation was modeled at a flat rate of 0.4% per hour. The block capacity tariff design is based upon the design that produced the best results in [34], with C_{bar} set at 75% of the annual load peak, C_{p1} at 0.0584 €$/kW$ and C_{p2} at 0.1872 €$/kW$. This block capacity design is compared to a fixed capacity tariff of 0.0652 €$/kW$, and a case without a capacity tariff; see fig. 4 for a visual representation of a block capacity tariff. In the simulations where intermittent generation is part of the simulated microgrid, this was modeled as 2.1 kWp of PV generation, to represent a modal Belgian household with PV generation. The stopping criteria for the heuristic are maximum 1000 optimization iterations per time window and a precision of 0.01 €.

Both cases with and without a capacity tariff are simulated for system con-

figurations with and without the inclusion of solar PV, resulting in four different set-ups. Each of these set-ups is then solved with each of the five different bases outlined above. The four different set-ups are also solved using bases with reduced dimensionality, based on the Walsh basis and the two Hadamard bases. Each of the mentioned simulations is executed for five different realizations of the same year, providing insight into the robustness and stability of the obtained results.

The exogenous datasets used in the simulations are all sourced from various Belgian electricity market actors: the consumer load is based on the synthetic load curves provided by Synergrid [31], the belgian federation of electricity- and natural gasgrid operators, while the electricity price profile used was obtained form EPEX SPOT Belgium [32], the Belgian power exchange operator. The intermittent generation in the simulation is provided by solar PV for which hourly generation data for Belgium is provided by the Belgian TSO, Elia [33].

3. Results and discussion

First, the results of the simulations using the five different bases are presented and discussed. Building upon this discussion, a second subsection details how the bases with reduced dimensionality are derived from the five original bases. The outcome of the simulations using the resulting bases is then discussed in the final subsection.

3.1. Results without dimensionality reduction

Tables 1 to 5 show the results of the simulations that were run. The results are grouped by simulation set-up: for example, table 1 reports the results for a microgrid without solar PV that is operating under a regime of block capacity pricing, listing the results of the two implemented heuristics for all of the considered bases. The outcomes are evaluated from both an economical as well as a technical point of view. The total average yearly operating cost is used as a metric for economic performance. Where technical performance is concerned, two

seperate, but closely related metrics are used. They are the average of the yearly peak capacity usage, taking into account both withdrawals from and injections into the grid, on the one hand and the crest factor, defined as the ratio between the peak capacity usage and the RMS value of the capacity usage over the year, on the other hand. The total yearly operating cost provides insights into the simulation outcomes where the private owner or operator of the microgrid is concerned, while the peak capacity used and the crest factor shed light on the effect of the capacity tariffs investigated on grid usage. The peak capacity usage and the crest factor provide similar, but distinct information: the peak capacity usage is straightforward, and shows peak usage of the electrical network by the microgrid, while the crest is a measure of "peakiness" in the capacity usage, as it provides information on the ratio of the highest capacity peak to the average capacity used. In terms of the grid, it also correlates with the utilization of assets that make up the distribution grid. In each table, the best results for all considered metrics are printed in boldface for each of the used heuristics.

A trend evident across all runs is that the solutions obtained for a bases with dimensionality 16 consistently outperform the problem formulations with dimensionality 24 of the same problem, except in the two fixed capacity pricing scenarios. In the case of fixed capacity pricing without solar PV, the results of the three non-standard bases are very close together, as show in table 3. The overall better performance of dimensionality 16 bases seems to indicate that from a computational point of view it is better to solve a larger number of smaller problems, as opposed to a smaller number of larger problems. However, when comparing the average yearly peak usage across all simulations ran, it is clear that the simulations with a twenty-four hour decision horizon have on the whole lower capacity usage peaks than the corresponding simulations with a sixteen hour decision horizon, the reason being that the base twenty-four representations have more hours to smooth out any demand or supply peak.

Furthermore, only in one of the twelve investigated cases is the best per-

forming algorithm one that is using the standard basis, as table 2 shows that the heuristic using the standard 16 base obtains the lowest cost in a system with solar PV, operating under block capacity pricing. Across all different system set-ups and heuristics, the Hadamard 16 base is the best performing of different bases tried, reporting the lowest average operating costs in six out of twelve cases, while the Walsh 16 base obtains the lowest average costs in three out of twelve cases. On the one hand, this means that one of our research hypotheses, that the increase of frequency present in Walsh basis is a property which would allow the heuristic to find better solutions more quickly, is not upheld. On the other hand, these results do show that another part of the research hypotheses is upheld: the non-standard bases outperform the standard bases.

Table 5 deserves special attention, as at first glance the results reported therein in both the Hadamard bases as well as the Walsh basis seem almost erroneous. However, when the pattern of electricity bought from and sold to the grid is examined, it is clear that these solutions engage in almost perfect price arbitrage, by buying up and storing grid electricity when the price is low in order to sell this electricity back to the grid when the price is high. Consequently, the grid is heavily used in this case, as doing so is free, meaning that the only price signal the system responds to, is the electricity price. Comparing these results to the results obtained with block or fixed capacity pricing also immediately proves the role that capacity tariff can play in stabilizing the grid, by limiting excessive buying and selling of electricity solely to exploit arbitrage opportunities. Capacity tariffs act as transaction costs, rendering hour to hour arbitrage based on minor price differences no longer profitable.

In a similar vein, the usefulness of capacity pricing is also demonstrated by comparing the results with and without the addition of solar PV for the three different capacity payment schemes, as they clearly show that different kinds of capacity tariff lead to the electricity generated by the PV panels being used in a different way. As can be expected, tables 5 & 6 show that most of the

electricity generated by the solar panels is sold to the grid in the case where there is no capacity tariff. This drives down the average yearly operating cost, while significantly heightening the capacity usage peak. Conversely, tables 1 & 2 show that the addition of solar PV has a much more nuanced impact on the behavior of the system under a system of block capacity pricing: here there is a slight increase or decrease of the peak capacity usage. As evidenced by tables 3 & 4, a fixed capacity tariff leads to an outcome in between these two extremes.

Furthermore, table 5 also shows the effectiveness of solving the economic dispatch problem using one of the proposed non-standard bases: the algorithm using these representations is able to find and exploit these arbitrage opportunities within the limited number of iterations available, whereas the same algorithm solving the same problem using a standard problem representation is not.

When comparing the average yearly operating cost between the three different capacity tariff schemes, fixed capacity pricing and block capacity pricing are quite close together, while system with no capacity tariffs predictably results in much lower operating costs. However, this favorable individual outcome is offset by heavy use of the electrical grid. While an investigation of this resulting externality is outside the scope of this study, this is clearly an unfavorable outcome for society. The choice between fixed capacity pricing or block capacity pricing is more interesting: consumers without solar PV are slightly better off under a block capacity scheme than under fixed capacity pricing, while the reverse is true for consumers with solar PV. As can be seen from fig. 4, block capacity pricing is cheaper than fixed capacity pricing as long as the capacity barrier is not heavily exceeded. It is only for capacity usage consistently exceeding the capacity barrier that fixed capacity pricing becomes cheaper for the consumer than block capacity pricing. Applied to the reported results, this means that under block capacity pricing, the system stay close enough to or below the capacity barrier so that the total yearly operating costs is lower than in the case

Block capacity pricing & no solar PV			
Basis	Av. cost	Peak	
Standard 16	514.30 (2.46)	5.65 (0.41)	12.00 (0.90)
Standard 24	518.56 (2.49)	5.65 (0.59)	11.98 (1.30)
Hadamard 16	**510.98** (1.70)	**3.45** (0.62)	**7.36** (1.36)
Hadamard 24	517.11 (2.04)	3.88 (0.38)	8.27 (0.80)
Walsh 16	511.32 (1.88)	4.01 (1.28)	8.53 (2.72)

Table 1: Simulation results under block capacity pricing for a microgrid without solar PV. 'Av. cost' stands for 'Average yearly operating cost' in Euro. 'Peak' represents the average of the maximum grid usage in kW and 'Crest' denotes the crest factor. For Av. cost, Peak & Crest, the standard deviation is reported in between brackets.

with a fixed capacity tariff. The addition of solar PV to the system, however, means that there is an excess of energy to be sold to the grid, driving up capacity usage, resulting in more capacity payments under a block tariff scheme than under a fixed capacity payment scheme.

The crest factors mimic the behavior of the peak capacity usage, in that a low peak capacity usage will generally also correspond to a low crest factor. When comparing the scenarios with and without solar PV, how the crest factor changes depends on the basis used for both block capacity pricing and fixed capacity pricing: adding solar PV drives the crest factor down for the simulations using the standard bases, and increases the crest factor for the non-standard bases.

As before, the two system configurations running without any kind of capacity tariff stand out: compared to the other cases their crest factor is low. While this does mean that the capacity demand of the microgrid is rather constant throughout the year, the peak capacity usage in these two cases are the highest amongst the investigated cases. Taken together, this means a constant, heavy load on the distribution network, which can have repercussions to those components susceptible to wear and tear.

Block capacity pricing & solar PV			
Basis	Av. cost	Peak	Crest
Standard 16	**202.85** (3.98)	4.09 (0.42)	7.78 (0.61)
Standard 24	211.16 (3.25)	**3.82** (0.33)	**7.03** (0.61)
Hadamard 16	221.35 (4.73)	4.60 (1.72)	8.44 (2.69)
Hadamard 24	225.15 (3.46)	4.54 (0.34)	8.09 (0.60)
Walsh 16	221.24 (4.08)	4.57 (1.29)	8.38 (2.35)

Table 2: Simulation results under block capacity pricing for a microgrid with solar PV. 'Av. cost' stands for 'Average yearly operating cost' in Euro. 'Peak' represents the average of the maximum grid usage in kW and 'Crest' denotes the crest factor. For Av. cost, Peak & Crest, the standard deviation is reported in between brackets.

Fixed capacity pricing & no solar PV			
Basis	Av. cost	Peak	Crest
Standard 16	523.21 (0.52)	6.53 (0.22)	12.33 (0.41)
Standard 24	528.16 (0.48)	6.06 (0.40)	11.57 (0.78)
Hadamard 16	520.62 (0.69)	5.54 (0.57)	9.80 (1.03)
Hadamard 24	**519.11** (0.56)	5.54 (0.46)	8.99 (0.72)
Walsh 16	520.53 (0.61)	**5.09** (0.60)	**8.98** (1.04)

Table 3: Simulation results under fixed capacity pricing for a microgrid without solar PV. 'Av. cost' stands for 'Average yearly operating cost' in Euro. 'Peak' represents the average of the maximum grid usage in kW and 'Crest' denotes the crest factor. For Av. cost, Peak & Crest, the standard deviation is reported in between brackets.

Fixed capacity pricing & solar PV			
Basis	Av. cost	Peak	Crest
Standard 16	187.04 (0.95)	6.07 (0.54)	8.91 (0.83)
Standard 24	201.82 (1.66)	6.39 (0.29)	9.19 (0.44)
Hadamard 16	186.76 (0.89)	6.32 (0.69)	9.29 (0.99)
Hadamard 24	**181.72** (1.30)	**5.93** (0.66)	**8.54** (0.93)
Walsh 16	186.96 (0.97)	7.08 (0.83)	10.40 (1.18)

Table 4: Simulation results under fixed capacity pricing for a microgrid with solar PV.'Av. cost' stands for 'Average yearly operating cost' in Euro. 'Peak' represents the average of the maximum grid usage in kW and 'Crest' denotes the crest factor. For Av. cost, Peak & Crest, the standard deviation is reported in between brackets.

No capacity pricing & no solar PV			
Basis	Av. cost	Peak	Crest
Standard 16	190.79 (2.11)	6.44 (0.22)	4.77 (0.13)
Standard 24	216.74 (1.59)	**6.37** (0.34)	5.43 (0.29)
Hadamard 16	**18.01** (2.08)	7.53 (0.10)	2.41 (0.04)
Hadamard 24	74.11 (2.04)	7.50 (0.09)	3.31 (0.03)
Walsh 16	18.09 (2.37)	7.52 (0.06)	**2.41** (0.02)

Table 5: Simulation results under no capacity pricing for a microgrid without solar PV.'Av. cost' stands for 'Average yearly operating cost' in Euro. 'Peak' represents the average of the maximum grid usage in kW and 'Crest' denotes the crest factor. For Av. cost, Peak & Crest, the standard deviation is reported in between brackets.

No capacity pricing & solar PV			
Basis	Av. cost	Peak	Crest
Standard 16	-161.87 (1.04)	8.76 (0.46)	5.76 (0.30)
Standard 24	-134.30 (0.85)	**7.88** (0.36)	5.85 (0.24)
Hadamard 16	-333.44 (2.76)	9.32 (0.39)	2.93 (0.12)
Hadamard 24	-277.33 (2.26)	8.56 (0.39)	3.64 (0.15)
Walsh 16	**-333.95** (2.87)	9.30 (0.22)	**2.86** (0.10)

Table 6: Simulation results under no capacity pricing for a microgrid with solar PV.'Av. cost' stands for 'Average yearly operating cost' in Euro. 'Peak' represents the average of the maximum grid usage in kW and 'Crest' denotes the crest factor. For Av. cost, Peak & Crest, the standard deviation is reported in between brackets.

3.2. Dimensionality reduction

The simulation results reported above were used as a starting point for reducing the dimensionality of the bases. In order to achieve this, the obtained solutions for each of the different simulation set-ups and bases are projected on their respective bases and squared. The average of these squares across the simulated year is taken and represents a measure for the relative importance of the corresponding basis vector in the solutions encountered. Additionally, we normalized the vector containing these weights for each of the bases to allow for comparison between bases. The bases with reduced dimensionality are constructed by retaining the twenty-five percent of basis vectors with the highest weights. The choice to retain a quarter of the basis vector is based on the results reported in fig. 5c, as the four basis vector with the highest weights are clearly distinguishable from the other basis vectors. In order to have comparable results, the same ratio was used on the two other bases. This dimensionality reduction is not carried out for the two standard bases, as dimensionality reduction in their case would imply that there would only be a non-zero solution for one quarter of the hours of the considered horizon.

The bases' components retained are columns 1,9,5 and 13 for the Hadamard 16 matrix, columns 1,13,19,7,20 and 4 for for the Hadamard 24 matrix and columns 1,2,3 and 4 for the Walsh matrix; these components then construct the dimensionally reduced bases. Note that the dimensionally reduced bases are ordered based on the calculated weights. Fig. 5 shows the result of this operation. It is immediately apparent that the choice of which basis vectors to retain is only dependent upon the choice of basis: fig. 5 shows that neither the system configuration nor the heuristic used have any impact on which of the basis vectors will be retained. While the weights of the first and second most important basis vector might shift a bit between different system set-ups, their respective position does not change. Additionally, the weights vary little in between different realizations of the same system configuration, as the marks of the same color are superimposed on one another in fig. 5.

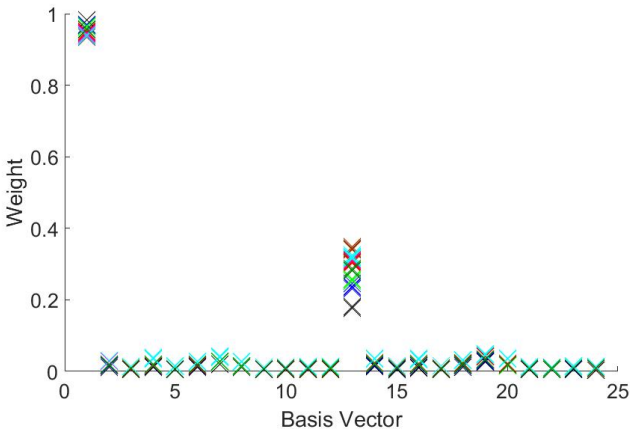

(a) Hadamard 24

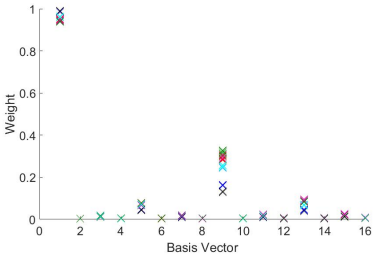

(b) Hadamard 16

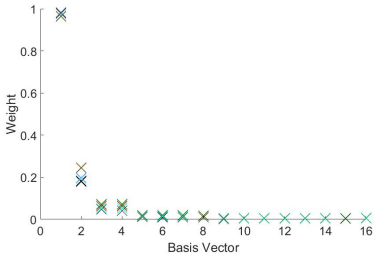

(c) Walsh 16

Figure 5: Normalised weights of the basis vector, grouped per basis. Colour codes are the same for all subfigures:
Red: Best improvement, block capacity pricing & no solar PV.
Blue: Best improvement, no capacity pricing & no solar PV.
Black: Best improvement, no capacity pricing & solar PV.
Green: Best improvement, block capacity pricing & solar PV.
Brown: First improvement, block capacity pricing & no solar PV.
Magenta: First improvement, no capacity pricing & no solar PV.
Cyan: First improvement, no capacity pricing & solar PV.
Dark Green: First improvement, block capacity pricing & solar PV.

3.3. Results with dimensionality reduction

In order to evaluate the impacts of using these dimensionally reduced bases on the yearly operational cost, the experiments were rerun using the dimensionally reduced bases. The scenario without a capacity tariff was not simulated again because of the high externalities that resulted from this scenario.

As is immediately apparent from comparing the results reported in tables 7 to 10 with their respective counterparts without dimensionality reduction, the performance of the heuristic after dimensionality reduction is highly dependent on the simulation set-up. The heuristic using the dimensionality reduced bases outperforms the full dimensionality bases for the case of a system without PV operating under a block capacity tariff scheme, and almost reach the same performance for a system without PV operating under fixed capacity tariffs. In both simulation set-ups incorporating solar PV, the dimensionally reduced bases are outperformed by the heuristic using the full dimensionality bases.

As can be seen from tables 7 and 9, the heuristics using the dimensionally reduced bases manage to keep the peak capacity usage down. Tables 8 and 10 show a similar, but less pronounced, reduction of peak capacity usage for the system configurations with solar PV generation. The crest factors exhibit a similar behavior.

Looking at the results for the dimensionally reduced bases, it is now the Walsh base that presents the low average cost overall. It is the cheapest in six out of eight of the simulation configurations ran, while being well within 1 standard deviation from the best performing algorithm in the two other cases. This reversal from the results discussed in section 3.1 shows that the Walsh 16 basis is the most suited of the bases for the dimensionality reduction outlined above.

The main reason for the higher yearly operating costs prevalent among the

simulations using the dimensionally reduced bases is that they no longer have the flexibility to fully make use of the arbitrage operations offered by the real-time energy market, precisely because of the reduction of dimensionality in the bases used. These higher average yearly operating costs are however offset by a reduction in computation time: while comprehensive and comparable data on run times is not available as the simulations were run in parallel on different computers, computation time for the instances on one of the used machines dropped from 950 seconds to 550 seconds when switching to the dimensionally reduced base representations of the problem, meaning that the dimensionality reduction certainly has its merits.

Using the dimensionally reduced bases, it is also possible to clearly show another advantage of using a capacity tariff, as it impacts the charge-discharge behavior of the battery. The number of charge-discharge cycles can be approximated by counting the number of sign changes in the power flow from the battery, with every pair of consecutive sign changes corresponding with a charge-discharge cycle. This is however an approximation which will overestimate the true number of cycles, as a certain depth of discharge is required before such cycling affects the useful lifetime of the battery. When looking at this charge-discharge behavior, the heuristic using the Walsh 16 basis performs best across the board, obtaining the results outlined in this section with between 1100 and 1650 charge-discharge cycles. The dimensionally reduced version of this Walsh 16 basis, however, only needs between 600 and 900 charge-discharge cycles, with comparable reductions for both of the Hadamard bases. While the technical specifics of the impact of number and type of charge-discharge cycles on expected battery lifetime is outside the scope of this paper, it is to be expected that such a drastic reduction in the number of charge-discharge cycles per year will have a positive impact on the overall lifetime of the battery. This effect could, at least partially, offset the reported difference in yearly operating cost between the normal and dimensionally reduced versions of the algorithm. A more detailed analysis of the actual battery technology used would be required

Block capacity pricing & no solar PV			
Basis	Av. cost	Peak	Crest
Hadamard 16	**509.63** (1.63)	1.67 (0.12)	3.54 (0.26)
Hadamard 24	513.75 (1.75)	**1.39** (0.07)	**3.00** (0.16)
Walsh 16	509.65 (1.55)	1.66 (0.05)	3.46 (0.20)

Table 7: Simulation results under block capacity pricing for a microgrid without solar PV, using dimensionally reduced bases. 'Av. cost' stands for 'Average yearly operating cost' in Euro. 'Peak' represents the average of the maximum grid usage in kW and 'Crest' denotes the crest factor. For Av. cost, Peak & Crest, the standard deviation is reported in between brackets.

Block capacity pricing & solar PV			
Basis	Av. cost	Peak	Crest
Hadamard 16	255.39 (4.43)	**3.07** (0.26)	**5.33** (0.45)
Hadamard 24	262.80 (5.27)	3.81 (0.76)	6.00 (0.66)
Walsh 16	**255.01** (4.60)	3.43 (0.45)	5.95 (0.77)

Table 8: Simulation results under block capacity pricing for a microgrid with solar PV, using dimensionally reduced bases. 'Av. cost' stands for 'Average yearly operating cost' in Euro. 'Peak' represents the average of the maximum grid usage in kW and 'Crest' denotes the crest factor. For Av. cost, Peak & Crest, the standard deviation is reported in between brackets.

to address this question.

4. Conclusion

We have solved the day-ahead economic dispatch problem for a microgrid with storage and local intermittent generation and with the inclusion of capacity tariffs. We used our own multi-start heuristic to solve this problem, and showed

Fixed capacity pricing & no solar PV			
Basis	Av. cost	Peak	Crest
Hadamard 16	545.73 (0.45)	2.64 (0.16)	5.28 (0.31)
Hadamard 24	557.71 (0.43)	2.80 (0.03)	6.37 (0.07)
Walsh 16	**524.52** (0.41)	**1.77** (0.06)	**3.33** (0.12)

Table 9: Simulation results under fixed capacity pricing for a microgrid without solar PV, using dimensionally reduced bases.'Av. cost' stands for 'Average yearly operating cost' in Euro. 'Peak' represents the average of the maximum grid usage in kW and 'Crest' denotes the crest factor. For Av. cost, Peak & Crest, the standard deviation is reported in between brackets.

Fixed capacity pricing & solar PV			
Basis	Av. cost	Peak	Crest
Hadamard 16	265.04 (0.45)	**3.76** (0.07)	4.83 (0.09)
Hadamard 24	289.40 (0.87)	3.59 (0.11)	**4.58** (0.14)
Walsh 16	**197.61** (0.58)	**3.15** (0.16)	5.26 (0.30)

Table 10: Simulation results under fixed capacity pricing for a microgrid with solar PV, using dimensionally reduced bases. 'Av. cost' stands for 'Average yearly operating cost' in Euro. 'Peak' represents the average of the maximum grid usage in kW and 'Crest' denotes the crest factor. For Av. cost, Peak & Crest, the standard deviation is reported in between brackets.

our heuristic approach to be effective. Our results have both methodological and policy implications.

Where the methodology is concerned, our results show that using a representation which mimics some of the periodicity inherently present in the problem being studied has benefits, as evidenced by the strong performance of the non-standard bases used. Furthermore, we have shown that these non-standard bases can be used to reduce the dimensionality of the problem, thereby saving on computational time: a dimensionality reduction of 75% corresponded to a runtime reduction of 40% and a cost increase of 20%, clearly showing that the dimensionality reduction has merit.

We have also shown how it is possible to steer consumer load with both energy and capacity price signals. Our results show the impact of the design of the capacity tariff on the load behaviour of consumers: a block capacity tariff is able to limit peak capacity usage more than a fixed capacity tariff scheme, which is in accordance with the results earlier published by Fridgen et al. [35], while at the same time leading to comparable cost outcomes for the consumer. While these results may not seem that surprising, given that capacity tariffs have been shown to promote flexibility in power to heat applications, our results clearly show that capacity tariffs can also be effective in encouraging battery uptake.

It should be noted that the main limitation of this research is the limited

amount of tested capacity tariff designs. The design itself of the proposed capacity tariff could be altered, by incorporating more blocks or by using a continuous cost function. However, this would mean complicating the tariff design, which seems hard to justify: the proposed two-block design performs well. Similarly, different set-points, both for the cut-off between capacity block one and two as well as for the price of capacity within each block could be investigated. This would reveal how these parameters influence both the operation of the system as well as the resultant cost. While this is certainly a worthwhile question, it is probably better tackled as part of follow-up research, where not only these parameters are changed, but the system configuration is varied as well. Such a study would then explore if a single tariff design fits all, or if different kinds of prosumers would need or benefit from different tariff designs, which seems to be a promising avenue of further research.

The resulting recommendation for policy makers is clear. Given the fact that storage is deemed a vital component in an energy supply system with a high percentage of renewable generation, an energy tariff system which includes a capacity component should be strongly considered. Such a tariff system will prove far more efficient at promoting the installation of energy storage systems, as opposed to strictly volumetric systems. Moreover, a block capacity tariff will also generate societal benefits, since it allows for a distribution network which will serve similar amounts of energy to end users with less infrastructure. This in turns means that the existing infrastructure can be used longer, leading to investment deferral.

5. References

[1] IEEE Smartgrid [Internet], IEEE joint task force on quadrennial energy review, Utility and Other Energy Company Business Case Issues Related to Microgrids and Distributed Generation (DG), Especially Rooftop Photo-

voltaics, Presentation to the U.S. Department of Energy 2014, on the www, url: https://smartgrid.ieee.org/images/files/pdf/IEEE_QER_Microgrids_October_3_2014.pdf.

[2] Milis K., Peremans H., Van Passel S. *The impact of policy on microgrid economics: A review*, Renew. and Sustain. Energy Rev. 2018;81.2;3111-19.

[3] Kempener R., De Vivero, G. *Renewables and energy storage: a roadmap for REmap 2030*, IRENA 2015.

[4] A. Cagnano, A. Caldarulo Bugliari, E. De Tuglie *A cooperative control for the reserve management of isolated microgrids*, Appl. Energy 2018;218;256-65.

[5] Quashie M., Marnay C., Bouffard F., Joós G. *Optimal planning of microgrid power and operating reserve capacity*, Appl. Energy 2018;210;1229-36.

[6] Makrygiorgou D., Alexandridis A. *Distributed stabilizing modular control for stand-alone microgrids*, Appl. Energy 2018;210; 925-35

[7] Cucuzzella M., Lazzari R., Trip S., Rosti S., Sandroni C., Ferrara A. *Sliding mode voltage control of boost converters in DC microgrids*, Control Eng. Pract. 2018;Volume 73;161-70.

[8] Xu Z., Yang P., Zheng C., Zhang Y., Peng J., Zeng Z. *Analysis on the organization and Development of multi-microgrids*, Renew. and Sustain. Energy Rev. 2018;81.2;2204-16.

[9] Shakya B., Bruce A., MacGill I., *Survey based characterisation of energy services for improved design and operation of standalone microgrids*, Renew. and Sustain. Energy Rev. 2019;101;493-503.

[10] Mengelkamp E., Gärttner J., Rock K., Kessler S., Orsini L., Weinhardt C. *Designing microgrid energy markets: A case study: The Brooklyn Microgrid*, Appl. Energy 2018;210;870-80.

[11] Zafar T., Zafar K., Zafar J., Gibson A. A. P.*Integration of 750MW renewable solar power to national grid of Pakistan âĂŞ An economic and technical perspective*, Renew. and Sustain. Energy Rev. 2016;59;1209-19.

[12] Zhao B., Chen J., Zhang L., Zhang X., Qin R., Lin X. *Three representative island microgrids in the East China Sea: Key technologies and experiences*, Renew. and Sustain. Energy Rev. 2018;96;262-74.

[13] Hirsch A., Parag Y., Guerrero J. *Microgrids: A review of technologies, key drivers, and outstanding issues*, Renew. and Sustain. Energy Rev. 2018;90;402-11.

[14] Yoldaş Y., Önen A., Muyeen S.M., Vasilakos A. V., Alan İ. *Enhancing smart grid with microgrids: Challenges and opportunities*, Revisiting feed-in tariffs in Australia: A review 2017;72;205-14.

[15] Siddiqui A., Marnay C., Edwards J.L., Firestone R., Ghosh S., Stadler M. *Effects of a carbon tax on microgrid combined heat and power adoption*, J. Energy Eng. 2005;131;2-25.

[16] Poruschi L., Ambrey C.L., James C.R. Smart J.C.R.,*Revisiting feed-in tariffs in Australia: A review*, Renew. and Sustain. Energy Rev. 2018;82.1;260-70.

[17] Atalay Y., Kalfagianni A., Pattberg P. *Renewable energy support mechanisms in the Gulf Cooperation Council states: Analyzing the feasibility of feed-in tariffs and auction mechanisms*,Renew. and Sustain. Energy Rev. 2017;72;723-33.

[18] Rious V., Perez Y. *Review of supporting scheme for island powersystem storage* Renew. and Sustain. Energy Rev. 2014;29;754-65.

[19] Bergaentzlé C., Jensen I.G., Skytte K., Olsen O.J. *Electricity grid tariffs as a tool for flexible energy systems: A Danish case study*, Energy Policy 2019;126;12-21.

[20] Sandberg E., Kirkerud J.G, Trømborg E., Bolkesjø T.F. *Energy system impacts of grid tariff structures for flexible power-to-district heat*, Energy 2019;168;772-781.

[21] DeForest N., Jason S. MacDonald J.S, Douglas R. Black D. R. *Day ahead optimization of an electric vehicle fleet providing ancillary services in the Los Angeles Air Force Base vehicle-to-grid demonstration*, Appl. Energy 2018;210;987-1001.

[22] Liu F., Bie Z., Liu S., Ding T. *Day-ahead optimal dispatch for wind integrated power system considering zonal reserve requirements*, Appl. Energy 2017;188;399-408.

[23] Crowston, W.B., Glover, F., Thompson, G.L., Trawick, J.D., 1963. Probabilistic and Parametric Learning Combinations of Local Job Shop Scheduling Rules. Technical Report 117. Carnegie-Mellon University, Pittsburgh.

[24] Hansen, P., Mladenović N. *First vs. best improvement: An empirical study*, Discret. Appl. Math. 2006;154;802-17.

[25] Ochoa G., Verel S., Tomasssini M. *Frist-improvment vs. Best-improvement Local Optima Networks of NK lanscapes*, Parallel Probl. Solving From Nat. 2010;104-113.

[26] Fathima A. H., Palanisamy K. *Optimization in microgrids with hybrid energy systems: A review*, Renew. and Sustain. Energy Rev. 2015;45;431-46.

[27] Sörensen K. *Metaheuristics - the metaphor exposed* Int. Trans. in Oper. Res. 2015;2;3-18

[28] Tenenbaum J. B., de Silva V., Langford J. C. *A global geometric framework for nonlinear dimensionality reduction*, Science 2000;290;2319-23

[29] Evins R. *A review of computational optimisation methods applied to sustainable building design*, Renew. and Sustain. Energy Rev. 2013;22;230-45

[30] Milis K., Peremans H., Van Passel S. *Steering the adoption of battery storage through electricity tariff design*, Renew. and Sustain. Energy Rev. 2018;98;2018;125-39.

[31] Synergrid, *Synthetic Load Profiles (SLP)* , on the www, url: http://www.synergrid.be/index.cfm?PageID=16896, last consulted on 15/09/2017 (in Dutch)

[32] Belpex, 2017 *Market Data Services*, September. On the www, url: https://www.belpex.be/servies/market-data-services.

[33] Elia, 2014. Solar-PV Power Generation Data, October. On the WWW, url: http://www.elia.be/en/grid-data/power-generation/Solar-power-generation-data.

[34] Schreiber M, Wainstein ME, Hochloff P, Dargaville R. *Flexible electricity tariffs: Power and energy price signals designed for a smarter grid*, Energy 2015; 93;2568-2581.

[35] Fridgen G., Kahlen M., Ketter W., Rieger A., Thimmel M. *One rate does not fit all: An empirical analysis of electricity tariffs for residential micro-grids*, Appl. Energy 2018;210;800-814.

Appendix A: Derivation of the objective function

Model with idealized battery storage in the time domain

Note that within each optimization window, the index is always renumbered, starting from 1 and ending at H. Expression (5) shows the objective function, while equations (6)-(8) show the constraints, for the case where an ideal battery, without discharge, is considered.

$$\min_{Q_g} \left[\sum_{t=1}^{H} Q_g(t) \cdot P_g(t) + |Q_g(t)| \cdot C_{p1} + max(|Q_g(t)| - C_{bar}, 0) \cdot (C_{p2} - C_{p1}) \right] \tag{5}$$

Subject to

$$Q_l(t) = Q_g(t) + Q_s(t) + Q_i(t), \quad \forall t = 1, \ldots, H \tag{6}$$

$$Q_{s,0} - \sum_{\tau=1}^{t} Q_s(\tau) \leqslant Q_{s,max} \quad \forall t = 1, \ldots, H \tag{7}$$

$$\sum_{\tau=1}^{t} Q_s(\tau) \leqslant Q_{s,0} \quad \forall t = 1, \ldots, H \tag{8}$$

The objective of the optimisation is to minimise the cost, over the considered horizon H, inured by buying electricity from the grid on the one hand and the capacity tariff payments due on the other hand, as show in Equation (5). Equation (6) enforces Kirchhoff's current law for the single node depicted in fig. 1: at all times, the load $Q_l(t)$ must be met through the sum of energy procured from the main grid $Q_g(t)$, the battery storage $Q_s(t)$, and possibly intermittent generation present in the microgrid $Q_i(t)$. Do note the signs for the energy flows as shown in fig. 1: all flows are considered positive when they flow towards the load. Where the battery is concerned, this means that discharging the battery will mean that $Q_s(t)$ is positive, while charging the battery will result in a negative sign for $Q_s(t)$. All the other constraints are constraints on the usage of the battery. Equation (7) corresponds to a set of H constraints, one for every hour of the considered H hour period, on charging the battery.

For each individual hour, the sum of the energy that was stored in the battery at the beginning of the optimization step, denoted by $Q_{s,0}$, plus the net inflow to the battery, up to the hour currently under consideration, cannot exceed the maximum storage capacity of the battery denoted by $Q_{s,max}$. Similarly, equation (8) is again a set of H constraints, but this time on the discharging of the battery: for each of the hours considered, the net energy outflows from the battery up to the hour under consideration cannot exceed the energy that was stored in the battery at the beginning of the period. Where the variables themselves are concerned, $Q_g(t)$ and $Q_s(t)$ need to be elements of $\mathbb{R}$, while $Q_i(t)$ and $Q_l(t)$ are elements of $\mathbb{R}^+$.

Model with a self-discharging battery in the time domain

In this section, the simple model (5)-(8) is refined by taking the self-discharge behaviour of the battery into account. Equations (5) and (6) remain valid, however, the two sets of constraints governing the charge and discharge behavior will have to be adapted. A battery storage component that exhibits self-discharging behavior can be modeled by the following dynamic model:

$$\frac{dS}{dt} = -Q_s(t) - l \cdot S(t) \tag{9}$$

In the continuous model defined by equation (9), $S(t)$ denotes the state of charge of the battery at time t, and l, for leakage, characterizes the rate of self-discharge. Solving the first order linear differential equation in (9) yields the expression for the state of charge at any given time t:

$$S(t) = Q_{s,0} \cdot e^{-l \cdot t} - \int_0^t Q_s(\tau) \cdot e^{-l \cdot (t-\tau)} d\tau \tag{10}$$

At all times the state of charge of the battery has to be positive, and is bounded by the maximum capacity of the battery:

$$0 \leqslant S(t) \leqslant Q_{s,max} \tag{11}$$

or

$$-Q_{s,0} \cdot e^{-l \cdot t} \leqslant -\int_0^t Q_s(\tau) \cdot e^{-l \cdot (t-\tau)} d\tau \leqslant Q_{s,max} - Q_{s,0} \cdot e^{-l \cdot t} \tag{12}$$

or

$$-Q_{s,0} \leqslant -\int_0^t Q_s(\tau) \cdot e^{l \cdot \tau} d\tau \leqslant Q_{s,max} \cdot e^{l \cdot t} - Q_{s,0} \tag{13}$$

Discretising equation (13) with a time-step of one hour in order to fit in with the rest of the model yields

$$-Q_{s,0} \leqslant -\sum_{\tau=1}^{t} Q_s(\tau) \cdot e^{l \cdot \tau} \leqslant Q_{s,max} \cdot e^{l \cdot t} - Q_{s,0} \quad \forall t = 1, \cdots, H \tag{14}$$

or, when split in to two inequalities:

$$Q_{s,0} - \sum_{\tau=1}^{t} Q_s(\tau) \cdot e^{l \cdot \tau} \leqslant Q_{s,max} \cdot e^{l \cdot t} \quad \forall t = 1, \cdots, H \tag{15}$$

and

$$\sum_{\tau=1}^{t} Q_s(\tau) \cdot e^{l \cdot \tau} \leqslant Q_{s,0} \quad \forall t = 1, \cdots, H \tag{16}$$

Equations (15) and (16) each represent H constraints, one for each of the hours comprised in the time window under consideration, on the charging and discharging of the battery respectively.

Model as expressed in terms of a general H-dimensional set of basis functions

The models build in the previous two sections are all written with the assumption that the problem is being worked on in the time domain. The set of H setpoints that are generated for the grid and the battery can also be seen as a single vector:

$$\bar{Q}_s = [Q_s(1), \cdots, Q_s(H)] \tag{17}$$

$$\bar{Q}_g = [Q_g(1), \cdots, Q_g(H)] \tag{18}$$

It is possible to reformulate the problem to make use of any H dimensional base consisting of basis vectors $\bar{b}_h$ and coefficients s_h and g_h , such that:

$$\bar{Q}_s = \sum_{h=1}^{H} s_h \cdot \bar{b}_h \tag{19}$$

$$\bar{Q}_g = \sum_{h=1}^{H} g_h \cdot \bar{b}_h \tag{20}$$

Substituting equations (19) and (20) into equations (15) and (16) yields:

$$Q_{s,0} - \sum_{\tau=1}^{t} \sum_{h=1}^{H} s_h \cdot \bar{b}_h(\tau) \cdot e^{l \cdot \tau} \leqslant Q_{s,max} \cdot e^{l \cdot t} \quad \forall t = 1, \cdots, H \tag{21}$$

$$\sum_{\tau=1}^{t} \sum_{h=1}^{H} s_h \cdot \bar{b}_h(\tau) \cdot e^{l \cdot \tau} \leqslant Q_{s,0} \quad \forall t = 1, \cdots, H \tag{22}$$

Equations (21) and (22) are the formulations of the constraints on the charging and discharging of the battery used in the final model. Rewriting the objective function and the first constraint leads to the final formulation of the optimisation problem that will be solved:

$$\min_{g_h} \left[\sum_{h=1}^{H} g_h \cdot \bar{b}_h \cdot \bar{P}_g + |\sum_{h=1}^{H} g_h \cdot \bar{b}_h| \cdot \bar{C}_{p1} + max(|\sum_{h=1}^{H} g_h \cdot \bar{b}_h| - \bar{C}_{bar}, 0) \cdot (\bar{C}_{p2} - \bar{C}_{p1}) \right] \tag{23}$$

Subject to

$$\bar{Q}_l = \sum_{h=1}^{H} g_h \cdot \bar{b}_h + \sum_{h=1}^{H} s_h \cdot \bar{b}_h + \bar{Q}_i \tag{24}$$

$$Q_{s,0} - \sum_{\tau=1}^{t} \sum_{h=1}^{H} s_h \cdot \bar{b}_h(\tau) \cdot e^{l \cdot \tau} \leqslant Q_{s,max} \cdot e^{l \cdot t} \quad \forall t = 1, \cdots, H \tag{25}$$

$$\sum_{\tau=1}^{t} \sum_{h=1}^{H} s_h \cdot \bar{b}_h(\tau) \cdot e^{l \cdot \tau} \leqslant Q_{s,0} \forall t = 1, \cdots, H \tag{26}$$

In equations (25) and (26), $\bar{b}_h(\tau)$ denotes the $\tau - th$ element of the $h - th$ basis vector. Additionally, all of the assumed exogenous variables in the model

have been rewritten as vectors for consistency. $\bar{P}_g$, $\bar{Q}_l$ and $\bar{Q}_i$ each contain H values of the corresponding dataset for each of the H hours of the considered time period, while $\bar{C}_{p1}$, $\bar{C}_{p2}$ and $\bar{C}_{bar}$ are all size H vectors, with all elements being equal to C_{p1}, C_{p2} and C_{bar} respectively. All the products in equation (23) between vectors are scalar products.